Quantitative in vivo dual-color bioluminescence imaging in the mouse brain

Markus Aswendt[1,2,*], Stefanie Vogel[1], Cordula Schäfer[1], Amit Jathoul[3], Martin Pule[4], Mathias Hoehn[1,5]

[1] In-vivo-NMR Laboratory, Max Planck Institute for Metabolism Research, Cologne, Germany
[2] University of Cologne, Faculty of Medicine and University Hospital Cologne, Department of Neurology
[3] Molecular Biosciences, Cardiff School of Biosciences, Cardiff, UK
[4] Department of Haematology, Cancer Institute, University College London, London, UK
[5] Department of Radiology, Leiden University Medical Center, Leiden, Netherlands

***Corresponding author:**
Markus Aswendt, PhD
University Hospital Cologne
Department of Neurology
Kerpener Strasse 62
50937 Cologne
Germany
+49 221 478-86416
markus.aswendt@uk-koeln.de

Abstract

Bioluminescence imaging (BLI) is an optical imaging method which can be translated from the cell culture dish in vitro to cell tracking in small animal models in vivo. In contrast to the more widely used fluorescence imaging which requires light excitation, in BLI the light is exclusively generated by the enzyme luciferase. The luciferase gene can be engineered to target and monitor almost every cell and biological process quantitatively in vitro and even from deep tissue in vivo. While initially used for tumor imaging, bioluminescence was recently optimized for mouse brain imaging of neural cells and monitoring of viability or differentiation of grafted stem cells. Here, we describe the use of bright color-shifted firefly luciferases (Fluc) based on the thermostable x5 Fluc that emit red and green for effective and quantitative unmixing of two human cell populations in vitro and after transplantation into the mouse brain in vivo. Spectral unmixing predicts the ratio of luciferases in vitro and a mixture of cells precisely for cortical grafts, however, with less accuracy for striatal grafts. This dual-color approach enables the simultaneous visualization and quantification of two cell populations on the whole brain scale with particular relevance for translational studies of neurological disorders providing information on stem cell survival and differentiation in one imaging session in vivo.

Keywords

spectral unmixing, luciferase, bioluminescence, stem cells, implantation, optical imaging

Introduction

Firefly luciferases (Flucs) are very efficient molecular and biochemical tools to track cells, proteins, and to monitor gene expression in living organisms [1]. While the first bioluminescence imaging (BLI) was limited to tumor applications [2], the firefly gene and the detection hardware were continuously optimized to monitor other cell types, such as stem cells and neurons, in deep tissue with higher or equal sensitivity and specificity compared to for example fluorescence imaging [3–8]. BLI has some unique advantages such as the light is produced directly in the Fluc expressing cells without the need of an excitation source, promoting a very low background and high signal-to-noise ratios (SNR). The efficiency of in vivo light production enables the detection of a minimal number of 1,500 to 3,000 neural stem cells (NSCs) engrafted to the mouse brain, through the intact skull, connecting tissue, and skin [9,10]. The survival rate of transplanted cells, which is an important factor to determine the outcome of translational stem cell studies, can be derived from the quantitative BLI signal, which requires adenosine triphosphate (ATP) for the luciferase enzyme reaction [11]. Furthermore, the luciferase gene was engineered to monitor the stem cell fate, for example the differentiation of stem cells into early neurons in vivo [12]. However, these measurements can be performed to-date only in separate, single color experiments. Multicolor BLI, the simultaneous imaging of two or more luciferases with distinct emission spectra, emerged first for in vitro assays and later for imaging bacteria or tumor cells in vivo [13–16]. Spectral unmixing an algorithm that can distinguish the spectral signatures is applied to extract the signal from two luciferases emitting light at different wavelengths and to calculates the respective contribution of each reporter on every pixel of an image [16,17].

The aim of this study was to probe spectral unmixing for bioluminescence neuroimaging with a focus on cell transplantation and to quantify the reliability of dual-color measurements. We describe experiments with a bright red-shifted [18,19] and a novel green-shifted point mutant of x5, a thermostable variant of wild type Fluc but with higher quantum yields [20,21]. This dual-color pair was chosen based on a comparison to other commonly used red/green Fluc mutants which showed efficient spectral unmixing in a cell assay in vitro. Furthermore, we provide for the first time a quantitative in vivo discrimination and unmixing-based estimation of two human neural stem cell populations in the mouse brain. Such multiplexed bioluminescence approaches will be useful to monitor the interaction of multiple cell populations in vivo and facilitate quantitative dual-color neuroimaging.

Results

In vitro spectral unmixing

Previously described variations of wildtype (WT) firefly luciferase (Fluc) containing 5 mutations (F14R, L35Q, V182K, I232K, F465R)[22] that reduce surface hydrophobicity and confer significant thermostability, were further mutated to red-shift (S284T) mutant x5red (x5r)[18] and to produce a novel blue-shifted (V241I/G246A/F250S) mutant x5green (x5g) bioluminescence spectra. In vitro, this novel dual-color Fluc pair was tested against the bioluminescence spectra of WT Fluc (Promega, Madison, WI, USA), PpyRE9 Fluc mutant [23], click beetle luciferase CBG99 [24], and Renilla luciferase hRluc [25] were acquired with the IVIS Spectrum CT system equipped with 18 emission filter (20 nm bandpass) at 37°C. Each luciferase was expressed by transfection of lentiviral vectors in the human tumor cell line HEK 293T. The bioluminescence signal was corrected for the co-expressed copGFP fluorescence measured separately with a plate reader. Here, copGFP levels reflect the transfection-based differences in luciferase expression due to a specific viral T2A linker in the bicistronic lentiviral plasmid providing equal expression levels of both transgenes. The normalized in vitro spectra [**Fig. 1**] show differences in peak photon emission as well as spectra shape. Notably, x5g produced in our setting the highest total photon flux (area under curve, AUC) compared to CBG99 and Luc2 (1.79- and 3.69-fold, respectively). For x5r, we found the AUC value to be 2.24-fold higher compared to PpyRE9 but only 0.45-times of the total photons from Luc2. The photon flux from cells expressing hRluc cannot be compared directly due to the different substrate (coelenterazine), however, the spectra clearly indicates the strong monophasic blue/green light emission. In contrast, emission spectra of firefly and click beetle luciferases follow a biphasic spline and in vitro/in vivo emission maxima of 520/560 nm (x5g, CBG99), 560/620 nm (PpyRE9, x5r) and 560/600 nm (Luc2). The spectral separation is higher for x5g/x5r for all measured wavelengths compared to the other green/red couples CBG99/PpyRE9, x5g/Luc2, and CBG99/Luc2. The second-best separation is achieved by combining x5g and Luc2.

As the next step, we performed spectral unmixing of HEK 293T cells transfected with x5g or x5r Fluc [**Fig. 2(a)**]. With the automated spectral unmixing algorithm provided by the IVIS software, the green and red emission spectra of x5g and x5r were extracted [**Fig. 2(b)**] and used for prediction of the x5g/x5r ratio in different mixtures [**Fig. 2(c)**]. The quantitative analysis of the unmixing data revealed high accuracy of predicted x5g ratios in relation to the actual number of plated x5g cells [**(Fig. 2(d)**]. A linear regression analysis showed that for both spectra, the unmixed photon counts are in linear relationship to the amount of Fluc cells for both reporters, x5g and x5r (R^2=0.991 *p<0.001* and R^2=0.994, *p<0.001*). For the predicting the correct x5g/r ratios, the algorithm results in a very low mean average deviation (MAD) of 0.02±0.02.

The influence of light absorption and scattering on the x5g/r Fluc photon emission was determined with a tissue-like blood agar mix consisting of gelatine, intralipid, and hemoglobin [**Fig. 3(a)**]. Plated x5g and x5r cells were covered with different amounts of the blood agar mix before imaging in order to mimic cell grafts implanted at different tissue depth. With increasing blood agar volume, the number of detected photons

decreased for x5r and x5g with an exponential two-phase decay [**Fig. 3(b)**]. The photon flux of x5g compared to x5r remained on average 1.79-fold higher independent of blood agar volume. Thus, under these in vitro conditions, no change in the x5g/r emission ratio was detected and no additional correction factor for the Fluc-specific absorption was calculated.

In vivo spectral unmixing

We determined the efficiency and accuracy of x5g and x5r Fluc unmixing in vivo by BLI of transfected HEK 293T cells which were transplanted into nude mouse brains and imaged on the following day. In comparison to other luciferases, x5g and x5r spectra exhibit substantial differences [**Fig. 4**]. The normalized spectra of x5g reveals in comparison to the green-shifted click beetle luciferase CBG99 at 560 nm a 2.07-fold higher photon flux. Thus, the green shoulder of the x5g spectrum is much more prominent. The differences between the two red-shifted firefly luciferases PpyRE9 and x5r in terms of total photon flux and shape of the spectrum are much less distinct.

In order to identify the influence of transplantation depth, we performed experiments with two separate groups: the cortical (-1.5 mm depth) as well as striatal (-3.0 mm depth) grafts. The experimental setting [**Fig. 5(a, d)**] included mice with x5r and x5g cells only as well as mice which received both cell types in in different mixtures. The two control mice were used to extract the in vivo x5r and x5g spectra from the cortex and striatum group in the auto unmixing mode, in which the software automatically detects x5r and x5g [**Fig. 5(b, e)**]. Notably, the total photon flux of x5g and x5r luciferase in the cortex is 1.93-fold and 1.76-fold higher compared to the striatum. The emission maximum of x5r is in both conditions at 620 nm but reached in the striatum only 58.44% photon flux of the photon flux of cortical grafts. In case of x5g, the spectrum in the striatal group is 20 nm shifted and the maximal photon emission only 41.98% of the cortex group. In the cortex group, automatic unmixing of the x5g ratio worked well with high accuracy for all expected x5g ratios ($F(4,13)=217.455$, $p<0.001$). A general comparison of expected to calculated x5g ratio resulted in a significant effect ($F(4,17)=79.961$, *p<0.001*), however, with stronger linear correlation compared to the striatum ($R^2=0.994$/*p<0.001* vs. $R^2=0.933$/*p=0.008*) [**Fig. 5(c, f)**]. A post-hoc comparison showed that for example the unmixing result is not precise enough to separate significantly cell grafts with 50 and 75% x5g cells, respectively (*p=0.179*). In order to further calculate the accuracy of unmixing, the linear regressions for cortical and striatal grafts were statistically compared to the implanted x5g ratios [Fig. 4(c, f)]. The difference between the slopes for cortical and striatal grafts were not significantly different (*p=0.319* and *p=0.450*). In addition, a one sample t test was calculated to compare the unmixing results with the known x5g ratio and the mean absolute deviation (MAD) was calculated to forecast the error in an experiment. For cortical and striatal grafts all unmixing ratios were not statistically significant different except of 100% x5g, which might be influenced by the small variation and sample size. The MAD for cortical grafts was smaller (4.5) compared to striatal grafts (8.0), supporting the observation that unmixing results and the expected x5g ratios were found to be very reliable for the cortex and less reliable for the striatum (**Table 1**).

We further processed the data assuming a scenario where the two control mice with x5g

and x5r cells for the auto unmixing mode are not present. The in vivo spectra and mean attenuation factors calculated from at 3 (cortex) or 4 (striatum) independent experiments were used to generate "library" spectra and to guide the unmixing algorithm [**Fig. 5(b, e)**]. In this case, the two control mice x5r and x5g would become obsolete. However, our calculations reveal less precise spectral unmixing for cortical and striatal grafts (**Table 1**). In the cortex group, statistically significant differences in x5g ratios were not predicted for 25 vs. 50 vs. 75% x5g cells in the mix. Most obvious is the strong under-representation of x5g in the mix especially for the striatal grafts which leads to false unmixing results, e.g. for 50% x5g in the striatum 23.0±4.1%, which is statistically significant different from the implanted 50% x5g cells. Similarly, the linear relationship for the increasing ratio of x5g cells in the mix holds true but with inferior correlation compared to the automated unmixing (cortex: R^2=0.939/*p=0.007*, striatum: R^2=0.856/*p=0.024*).

Table 1: Summary of in vivo unmixing validation.

	x5g%	Auto unmixing and pairwise comparison		One sample *t* test	MAD[1]	Library unmixing[2] and pairwise comparison		MAD[2]	One sample *t* test
Cortex	0	1.7±2.3	] *p=0.035**	*p=0.239*	1.7	0.9±1.0	] *p=0.032**	0.9	*p=0.120*
	25	21.5±9.9	] *p=0.009***	*p=0.607*	8.8	20.9±9.3	] *p=0.189*	8.3	*p=0.521*
	50	50.7±7.0	] *p=0.016**	*p*=0.922	5.5	46.0±7.0	] *p=0.100*	4.1	*p=0.270*
	75	65.0±4.1	] *p=0.003***	*p*=0.078	7.3	54.1±8.2	] *p=0.002***	20.9	*p=0.049**
	100	97.2±1.3		*p*=0.009**	3.3	90.8±6.1		9.2	*p=0.057*
Striatum	0	1.4±1.2	] *p=0.005***	*p=0.052*	1.3	1.9±2.5	] *p=0.018**	3.0	*p=0.203*
	25	18.0±8.1	] *p=0.001****	*p=0.125*	10.0	7.9±2.9	] *p=0.003***	14.7	*p=0.002***
	50	43.9±5.8	] *p=0.170*	*p=0.211*	6.2	21.0±4.1	] *p=0.182*	18.1	*p=0.005***
	75	55.7±16.5	] *p=0.007***	*p=0.179* *p=0.036**	19.3	28.1±13.2	] *p=0.005***	31.6	*p=0.006***
	100	96.9±2.2			3.2	96.5±4.6		3.7	*p=0.095*

[2]Mean absolute deviation. [1]Calculated with mean attenuation factor calculated from auto unmixing experiments: cortex x5r/x5g (5.99±2.46/10.99±6.85), striatum x5r/x5g (9.04±4.02/11.50±7.51). Statistical significance reported as p-value result of the t-test between a pair adjacent x5g ratios.

Discriminating two different neural stem cell populations

In order to further probe the spectral unmixing approach, we tested x5g in combination with the widely used Fluc Luc2 in neural stem cells (NSCs). The human H9-NSC line was stably transduced using EF1α-Luc2-T2A-copGFP or DCX-x5g-T2A-EGFP lentiviral vectors and sorted by FACS for their GFP expression, respectively (data not shown).

The resulting two stable transgenic cell lines were transplanted into the cortex of nude mice in the same mixture ratios as for the HEK 293T experiment (0/100, 25/75, 50/50, and 100/0% x5g/r) and imaged one and two days later [**Fig. 6(a)**]. The quantitative analysis revealed a linear correlation for both time points with a stronger correlation on the first day after transplantation [**Fig. 6(b)**]. The presence of the different cell types was verified by immunohistochemistry [**Fig. 6(c)**].

Discussion

We have recently characterized mutated luciferases originating from various species such as *Photinus pyralis* Fluc (Luc2, PpyRE9), *Pyrophorus plagiopthalamus* (CBG99), *Gaussia princeps* (Gluc), and *Renilla reniformis* (hRluc) for neuroimaging, which is particularly challenging, as the bioluminescent photons need to pass thick layers of bones and connective tissue. We further showed that spectral unmixing for CBG99 and PpyRE9 is possible also for deep tissue grafts, however, with limitation to qualitative analysis. [26] The aim of the present investigation was to optimize spectral unmixing for in vivo bioluminescent neuroimaging by using advanced green- and red-shifted Fluc mutants and characterize the accuracy to predict cell population ratios from quantitative unmixing results.

The conventional in vitro dual-luciferase assay combines Renilla and firefly luciferases [27]. These luciferases require different substrates (Fluc luciferin and Renilla coelenterazine), which makes the bioluminescent signal distinguishable. However, for many in vivo applications, the dual-luciferase approach is impractical because of the weak quantum yield, the absorption- and scattering-sensitive blue light emitted by Renilla, and it requires two separate imaging sessions. A different approach is spectral unmixing, a dissecting algorithm, which is able to partition bioluminescence signals originated from multiple fluorescence or luciferase sources into individual contributors [16,28]. Although spectral unmixing is widely used in fluorescence microscopy for cell imaging [29], in vivo applications - especially for neuroimaging - are technically challenging. It requires sensitive BLI detectors and engineered luciferases with distinct in vivo spectra. In a previous study, which was the first to compare reporter genes specifically for mouse brain applications, we found the Fluc Luc2 to be superior to other luciferases and the quantum yield (amount of photons emitted per luciferin molecule processed) to be more important than emission wavelength [30]. As we have shown here, tissue absorption and scattering have a significant impact on the luciferase spectrum, making the in vivo spectrum considerably different from that in vitro.

For our comparison, we have used the previously described red-shifted x5 mutant[18,19,31] and a novel green-shifted complement, x5g. They are based on a background that has improved thermo-stability, solvent stability, pH-tolerance in terms of activity, and resistance to bathochromic shift while retaining the same specific activity relative to the wild type [18,23,31]. As we could show here, x5g and x5r have superior quantum yields and a better spectral separation compared to the previously tested luciferases Luc2, PpyRE9, CBG99, and hRluc [30]. The comparison of emission spectra from luciferases expressed by HEK 293T cells in vitro and in vivo highlights the strong overlap of the other green- and red-shifted luciferases with Luc2. The benefit of using x5g/x5r for spectral unmixing compared to CBG99/PpyRE9 is a much stronger separation due to higher photon flux and difference in spectrum shape. Especially under in vivo conditions, the less pronounced attenuation of the green shoulder of x5g compared to CBG99

favors spectral separation also from deep tissue sources. Furthermore, the green-shifted x5g is 1.79- and 3.69-fold brighter than CBG99 and Luc. Likewise, x5r is 2.24-fold brighter than PpyRE9 [23,24] and the spectrum is characterized by a higher emission for wavelengths above 600 nm. Red-shifted probes are considered to be more efficient in vivo as light absorption in living tissue is negatively correlated with the emission wavelength [24,32,33]. However, the lower quantum yield of red-shifted luciferases has so far impeded sensitive detection of cell grafts in deep tissues, like the mouse brain [26]. The here tested x5r Fluc overcomes these limitations and was successfully validated for in vitro and in vivo spectral unmixing applications.

Under in vitro conditions, the dual-luciferase pair x5r/g provided the best spectral separation for all measured wavelengths compared to previously tested red and green-emitting luciferases [26]. In this line, the unmixing of different ratios of transfected HEK cells was straightforward with a minimal mean absolute deviation (MAD) of 0.02±0.02. There was a highly significant linear correlation between cell number and (unmixed) photon emission. In order to get reliable results, a simple correction factor compensating for the individual filter attenuation must be applied. This filter attenuation is the relation between the luciferase photon emission without filter vs. with filter and commonly used for in vitro dual-color luciferase assays [34]. We imaged a tissue-like phantom with Fluc-expressing cells covered with a blood and fat composition of human skin to model the in vivo situation of transplanted cells in the living animal. Under these conditions, the attenuation of photon emission due to increasing amounts of blood/fat follows an exponential curve for both, x5g and x5r, while the difference in total photon emission remains constant (x5g higher than x5r). According to that experiment, we did not calculate an addition correction factor. However, the in vivo emission spectra from x5g- and x5r-expressing HEK cells transplanted into the mouse brain revealed a strong tissue depth-dependent difference compared to the in vitro cell culture and tissue model. Total photon counts for x5g were much lower than for x5r. The total x5r photon counts were 5-fold and 1.8-fold higher compared to x5g cells in the cortex and striatum, respectively. The x5g peak emission was affected much stronger by tissue absorption compared to x5r, which is in agreement with other in vivo mouse brain studies using for example the red-shifted Fluc PRE9 [32]. Additional correction factors compensating for the Fluc-specific tissue absorption as determined for subcutaneous tumors in mice [35] would be an interesting target to further improve the quantification in future studies.

We found that the spectral unmixing algorithm works best when 2 “control” mice with x5g and x5r engrafted cells were present to allow an automatic detection of “pure” light from each luciferase. Although, the emission spectra were strongly influenced by tissue absorption and scatter, statistical measures proved that for cortical grafts and with less precision for striatal grafts quantitative unmixing is feasible. The mean absolute deviation (MAD) for cells implanted in the cortex of adult mice was very low (4.5) and the correlation of unmixing and actual x5g values followed a strict linear correlation which is statistically not different, providing sufficient quantitative calculations of various mixtures in dual-color imaging in vivo. In absence of both control mice, however, the automatic unmixing algorithm tends to extract unrelated red and green components of the spectra which may lead to wrong calculations of x5r/g ratio. The sampling of master spectra and an average for the filter attenuation from a batch of independent experiments resolved this problem only partially. In detail, we found less efficient unmixing for both, cortical and striatal grafts under those conditions of using library data. While unmixing with the

generated library data (master spectra) predicts the ratio of x5g qualitatively good for cortical grafts, it underestimates x5g in the striatal grafts. We speculate that the stronger absorption of the green part of the spectrum negatively influences spectral unmixing efficiency. Nevertheless, when sampled from more experiments, the library mode could be useful for in vitro and ex vivo measurement, respectively, making controls and/or additional animals with the pure green- and red-shifted luciferases obsolete.

Confounding factors for quantitative in vivo unmixing remain the biological variability in luciferin distribution, reporter gene expression and the stability of the image acquisition. Although the image acquisition was done in the steady-state of the luciferase activity (up to 30 min post luciferin injection [9]), a random order of emission filters would prevent an effect of lower/higher values related to the time after substrate injection. In order to probe our spectral unmixing strategy in a more difficult application, we transduced human NSCs with x5g and Luc2 constructs and transplanted different ratios into the nude mouse brain. The dual-color luciferase pair x5g/Luc2 was chosen as quantum yield and spectral separation are very similar to x5g/r. Furthermore, in this proof-of-concept example, the widely used luciferase Luc2 is controlled by the constitutive human EF1α promoter, which maintains Luc2 levels independent of NSC maturation state [12]. The x5g expression is driven by the DCX promoter and provides a second readout specific for early neurons. We could show that the dual-color luciferase approach is applicable to human NSCs and that spectral unmixing of in vivo BLI early after stem cell transplantation provides accurate and quantitative determination of undifferentiated vs. pre-differentiated cells. In our experiments, the estimation of x5g ratios in the mix was as good as for the HEK 293T cells at day 1 post implantation, but slightly worse the day after. This might be due to different cell death behavior of the two cell lines or varying DCX controlled reporter expression due to continuing neuronal differentiation. Due to technical limitations, we have used two GFP reporter, copGFP and EGFP, for both lentiviral vectors, which cannot be distinguished by fluorescence emission. In future experiments it will be necessary to mirror the red/green luciferase also with a set of equivalent fluorescent reporter to distinguish the cell types by histology. Notably, if a direct correlation of GFP to Fluc expression is needed, a measurement of the actual protein levels and the catalytic active protein, respectively, would be necessary [36]. The T2A linker regulates bicistronic expression and not protein stability. Furthermore, spectral unmixing should be tested with other improved pairs of luciferases and luciferins such as AkaLumine-HCl[8] with enhanced sensitivity for deep tissue imaging. With these technical improvements, imaging two different cell populations in the mouse brain at the same time has many important applications. In stem cell therapy of neurological disorders, for example, it could be used to monitor the viability and differentiation with two different colored luciferases in order to answer the question if the stem cell graft itself or an interplay of paracrine and immune-modulatory effects determine functional improvement.

Conclusion

Here, we have shown that spectral unmixing of dual-color bioluminescence reporter can determine the ratio of each luciferase. The unmixing was validated in human tumor and neural stem cells engrafted into the mouse brain cortex. Monitoring the expression of the two reporter genes by dual-color bioluminescence imaging holds great potential to advance luciferase-based in vitro and in vivo assays. It enables simultaneous imaging of

391 protein and cell interaction in health vs. disease condition and holds the potential to
392 advance stem cell fate imaging.
393

Material&Methods

Mutagenesis

Thermostable x5 Fluc contains 5 mutations (F14R, L35Q, V182K, I232K, F465R) that reduce surface hydrophobicity and confer significant thermostability[22]. The sequence of human codon optimised WT Fluc was constructed by gene synthesis by oligo assembly and the 5 mutations were added by splicing by overlap extension PCR-based cloning to produce the plasmid MP5556x5, cloned into SFG-retrovirus[37] upstream an internal ribosome entry site (IRES) and a truncated CD34 (dCD34) marker gene. Into this, mutations were added to either produce blue-shifted (V241I/G246A/F250S) and red-shifted (S284T) bioluminescence spectra in mutants x5green (x5g) and x5red (x5r), respectively.

Cell culture

The human embryonic kidney cell line 293T (HEK 293T) was cultured in DMEM+GlutaMAX medium (Life Technologies, Darmstadt, Germany) supplemented with 10% FBS (Life Technologies) and 1% Penicillin/Streptomycin (Life Technologies) under humidified conditions at 37 °C and 5% CO_2. Cells were passaged every 3 days and detached with Trypsin (Life Technologies). The human neural stem cell line H9-NSC (Life Technologies), which were initially derived from the human embryonic stem cell line H9 - NIH Registry WA09 [38] were maintained according to the manufacturer´s protocol. Briefly, cells were plated on Geltrex coating at a density of $5x10^4$ cells/cm^2 in StemPro NSC SFM complete medium consisting of 1x KnockOut DMEM/F-12, 2 mM GlutaMax, 20 ng/mL bFGF and EGF, and 2% StemPro supplement (Life Technologies). Cells were passaged every 3 days and detached with StemPro Accutase (Life Technologies).

Tissue-like phantoms

Tissue-like phantom was prepared as follows: 8.76 mg/mL hemoglobin (Sigma-Aldrich) and 40 mg/mL blood agar base (Sigma-Aldrich) were solved in 50 mM TBS buffer on a hotplate stirrer at 50 °C. When both components were dissolved, Lipovenös MCT (Fresenius Kabi, Bad Homburg, Germany) was added at a final concentration of 1%. For the construction of the tissue phantom, the 96-well plate with the attached transfected cells was placed on a 37 °C warming pad, the medium was removed, and the agar mixture was layered carefully above the cells in various volumes ranging from 0 to 175 µL.

Cell transfection and transduction

HEK 293T cells were transfected with the plasmids pcDH-EF1α-x5g-T2A-tdtomato+SV40Zeo or pcDH-EF1α-x5r-T2A-copGFP+SV40Zeo which consist of the constitutive promoter elongation factor 1 alpha (EF1α), the genetically engineered x5 Fluc red (+S284T) [18,19,31] and the novel green (+ V241I/G246A/F250S) mutant, the self-cleaving 2A-like peptide sequence from Thosea asigna virus (T2A), the green fluorescent protein copGFP from Pontellina plumata (Exc 482nm, Em 502nm) or the red fluorescent protein tdTomato (Exc 554nm, Em 581nm), the Simian virus 40 (SV40) origin, and a Zeocin resistance gene (Zeo). Molecular cloning of plasmids carrying Luc2,

CBG99, PpyRE9, and hRluc was described previously [26]. For this study, we designed novel bicistronic plasmids for constitutive and cell-specific expression of x5g and x5r by amplifying recombinant DNA by PCR using specific primers bearing appropriate restriction sites in the following steps. At first the backbone pcDH-EF1α-MCS-T2A-copGFP (System Biosciences, Mountain View, USA) was changed to pCDH-EF1α-MCS-T2A-tdTomato (pQC NLS TdTomato IX was a gift from Connie Cepko; Addgene plasmid #37347). In addition, we added the antibiotic resistance gene zeocin controlled by the independent SV40 promoter amplified from pBabe Zeo (pBABE zeo Ecotropic Receptor was a gift from William Hahn, Addgene plasmid #10687). Secondly, x5g or x5r were cloned with BamHI/NotI from M5556X5 or M5549X5 into pcDH-EF1α-MCS-T2A-tdtomato+SV40Zeo or pcDH-EF1α-MCS-T2A-copGFP+SV40Zeo. For the cell specific plasmids, fluorescence proteins were exchanged to tdTomato and EGFP (pmEGFP-1 was a gift from Benjamin Glick, Addgene plasmid #36409). The EF1α promoter was exchanged by the human DCX promoter (kind gift of Sebastien Couillard-Despres, Paracelsus Medical University, Salzburg, Austria) via ligation with the ClaI and XbaI restriction sites. The final plasmids used for transduction of H9-NSCs were: pcDH-EF1α-Luc2-T2A-copGFP and pcDH-DCX-x5green-T2A-EGFP. Successful cloning was verified by restriction analysis and sequencing.

For transient transfection, HEK 293T cells were seeded (71,400 cells/cm^2) on gelatine coated P60 cell culture dishes 12 h before transfection. Cells were transfected with 5.25 µg DNA and 10.5 µL Metafectene (Biontex, Munich, Germany) in 2 mL Opti-MEM medium (Life Technologies) and incubated for 4 h under normal conditions. Post transfection, cells were cultured for 2 to 3 days and prepared for in vitro dilution series or in vivo implantation.

Lentiviral vector-mediated transduction of H9-NSCs was performed using 3rd generation helper plasmids and subsequent cell incubation with unconcentrated pseudoviral particles for 24 h (for experimental details see [12]). We selected stably expressing cell lines based on the LTR-mediated background expression of EGFP and copGFP in the transduced cells via FACS (FACSAria III, BD Biosciences, San Jos, USA).

Cell Transplantation

All experiments were conducted according to the guidelines laid out in the German Animal Welfare Act and approved by the local authorities. Animals were kept in 12 h/12 h day/night cycle in individually ventilated cages. Food and water were offered ad libitum.

Cells transplantation was performed as described before [9]. Transfected HEK 293T cells were implanted individually or mixed (x5r:x5g; 1:1, 1:3 and 4:1) diluted with a final concentration of 150,000 cells/µL in HBSS (Life Technologies) and stored on ice until implantation. Cells were implanted into the right striatum (AP +0.5; L +2.0; DV −3.0 relative to bregma) or cortex (AP +0.5; L +2.0; DV −1.5 relative to bregma) of NMRI-Foxn1nu/Foxn1nu mice (age 9-11 weeks, 25–30 g, male from Janvier, Saint Berthevin Cedex, France). In total, we used 28 mice for cortical and 26 for striatal HEK 293T grafts of which 6 and 3, respectively, were excluded because of visual bleeding out of the bore hole.

In vitro and in vivo imaging set-up

Bioluminescence and fluorescence imaging experiments were performed with the IVIS Spectrum CT (PerkinElmer, Waltham, USA). We recorded emission spectra explicitly with the IVIS system as we used the system throughout all experiments and it was shown by Zhao and colleagues previously that recording emission spectra with the IVIS System results in comparable spectra acquired with a spectrophotometer [24].
For spectral unmixing of the in vitro dilution series respective cell numbers were diluted in PBS (Life Technologies) and plated on a black clear bottom 96-well plate (Sigma-Aldrich, Taufkirchen, Germany). D-luciferin potassium salt (Synchem, Felsberg, Germany) was solved in PBS and added in a final concentration of 1 mM (~0.3 mg/mL). Immediately after D-luciferin application, in vitro dilution series was imaged with following settings: FOV 13.2 cm, Excitation Block, Emission 500 to 840 nm (20 nm bandpass filter) and no filter (open filter setting), exposure time automatic, binning 8, f/stop 1. In addition, copGFP fluorescence was measured using the plate reader Mithras^2 LB943 (Berthold, Bad Wildbach, Germany) with the following settings: Excitation 469 nm, Emission 510 nm, lamp energy 40%, counting time 2.0 sec. In vivo BLI was performed one day post implantation. We used our mouse brain-adapted imaging protocol, which was described in detail elsewhere [9]. 50 mg/mL D-luciferin sodium salt (Synchem) was solved in PBS, sterile filtered, and injected intraperitoneally to each animal with a final dose of 300 mg/kg body weight before Isoflurane (ISO) anesthesia (2% ISO in 30% O_2/70% N_2O atmosphere). Image acquisition was started 8 min post D-luciferin injection for 25 min under following setting: FOV 22.5 cm, Excitation Block, Emission 500 to 840 nm with 20 nm bandwidth and open filter. The exposure time ranging from 1 to 60 sec, the lens aperture size, and the binning were set automatically by the system to reach the most sensitive setting. Finally, animals were sacrificed and brain tissues were processed for histology.

Immunostainings

For immunohistological staining of brain tissues, mice were transcardially perfused under ISO anesthesia with 20 mL PBS followed by 20 mL 4% phosphate buffered paraformaldehyde (PFA). Brains were removed and frozen in -40 °C cold 2-methylbutane and stored at -80 °C. Brains were cut in 14 µm thick sections in coronal plane with the cryostat (Leica, Wetzlar, Germany), mounted on object slides, and stored at -20 °C. To equilibrate tissue, brain sections were washed 3 times with PBS. Antigen retrieval was performed by incubating the brain sections in 10 mM sodium citrate buffer (pH 6.0) at 80 °C for 30 min. Unspecific antibody binding was reduced by blocking with 5% normal donkey serum and 0.25% Triton X-100 in PBS for 1 h. Primary antibodies were diluted with 0.25% Triton X-100 in PBS and incubated overnight at 4 °C. Brain sections were stained for mouse anti-HuNu (Chemicon, 1:200) and rabbit anti-copGFP (Evrogen, 1:200). Secondary antibodies – donkey anti-mouse-Cy5 (Jackson Immunoresearch, 1:200) and donkey anti-rabbit-Cy3 (Jackson Immunoresearch, 1:200) – were diluted with 0.25% Triton X-100 and Hoechst 33342 (Sigma-Aldrich, 1:000) in PBS and incubated for 2 h. Finally, brain sections were air-dried and mounted within Cytoseal XYL (Thermo Fisher Scientific).
All images were acquired with the BZ-9200 Microscope (Keyence, Neu-Isenburg, Germany). Representative images of the immunohistological staining were acquired with the 4x and 60x objectives and the respective phase contrast and fluorescence filter sets

(DAPI-BP, GFP-BP, TexRed, and Cy5 HC; Keyence).

Data analysis

Optical imaging data analysis and spectral unmixing was performed with the Living Image 4.3.1 software (PerkinElmer). Regions of interest (ROIs) with constant size were manually drawn for well plate quantification as well as in vivo data. Total photon flux was calculated as area under curve as described previously [9] and the filter with highest average radiance was selected as emission with maximum photon flux. The normalized as well as non-normalized master spectrum for x5g and x5r in the striatum or cortex were calculated by the average of 4 or 3 different acquisitions. The master spectrum was used in the "library" mode for spectral unmixing as guideline. The automatic ("auto") spectral algorithm was used whenever possible, or replaced by the (manual) guided unmixing in which the user has to pre-define where to find the pure x5g and x5r spectra. The data for the unmixed populations of x5g and x5r were corrected for the experiment-specific filter attenuation factor. This factor compensates for the difference between the average radiance of x5g/r unmixing at a certain filter (usual 600-620/620-640 nm) and the open filter (without filter) setting. Furthermore, this correction factor grades the experimental variability induced by the differences during transfection and transplantation. Without correcting for filter attenuation, the unmixing results will remain qualitative. The filter attenuation factor average of all processed cortical and striatal grafts was used for the master spectrum unmixing.

Histological images were processed with ImageJ 1.48s (National Institutes of Health, Bethesda, USA). Further calculations, plotting, and statistical analysis were done with MS-Excel 2010 (Microsoft Corporation, Redmond, USA) and SPSS 22.0 (IBM, Ehningen, Germany). For multiple group comparisons the one-way ANOVA with Welch statistics and post hoc pairwise comparison (Tukey-corrected) was used. A p-value ≤ 0.05 was considered to be significant. A Student's t-test was used for the comparison of experimental groups. The one sample t-test was used to compare unmixing results with the implanted x5g ratio. The mean absolute deviation (MAD) is the difference between actual values and the known values (implanted x5g cells). All values are expressed as mean ± standard deviation (SD) and statistical significance are indicated by *$p<0.05$, **$p<0.01$, ***$p<0.001$., # n.s.

Biographies

Markus Aswendt, PhD, received his MSc degree in 2009 and PhD in neurobiology from the University of Magdeburg and the Max Planck Institute in Cologne, Germany, in 2013 under Drs. Klaus Reymann und Mathias Hoehn. Following postdoctoral training in the lab of Dr. Gary Steinberg, Stanford University School of Medicine, USA, he was appointed a junior group leader in 2017 at the Department of Neurology, University of Cologne. His lab explores neuroimaging in mice to develop therapies for stroke.

Stefanie Vogel, PhD, received here MSc degree and PhD in biology from the University of Cologne, under Dr. Mathias Hoehn, Max Planck Institute for Metabolism Research, Cologne, Germany in 2018. Currently, she is a postdoctoral fellow at the Technical University Dresden, Germany, in the group of Dr. Jared Sterneckert.

Cordula Schäfer, is a technical assistant for molecular cloning and cell culture at the Max Planck Institute for Metabolism Research, Cologne, Germany.

Amit Jathoul, PhD, received his PhD in biotechnology and chemical engineering at the University of Cambridge, UK, in 2008. Following postdoctoral training with Martin Pule at the University College London, UK, he became a research fellow in the School of Biosciences at Cardiff University, UK, in 2016.

Martin Pule, PhD, received his Bachelor in Medicine and Surgery from the University College in Dublin, Ireland, in 1995. Following a Fulbright Scholarship at the Baylor College of Medicine, Houston, USA, he became a Senior Lecturer in Haematology at the University of London Cancer Institute, London, UK. He leads the optical imaging in the Center for Biological Imaging. He and his group work on engineering mammalian cells, especially T-cells, for therapeutic applications.

Mathias Hoehn, PhD, received his MSC degree in 1978 and PhD in biophysics at the University of Regensburg, Germany, in 1982. Following postdoctoral training at the University of California, San Diego, USA, in 1984, he was appointed head of the MRI group at the technical University of Aachen in 1985. Since 1987, he is leading the In-vivo-NMR lab at the Max Planck Institute for Metabolism Research in Cologne, Germany and was appointed a visiting professor in 2013 at the Leiden University Medical Center, The Netherlands.

Disclosure

None.

Acknowledgments

We acknowledge excellent technical assistance with histology and in vivo imaging from Anja Peglow and Andreas Beyrau. This work was financially supported by grants from the EU-FP7 programs TargetBraIn (HEALTH-F2-2012-279017) and BrainPath (PIAPP-GA-2013-612360). SV and MA were supported by a grant from the German research foundation DFG (AS-464/1-1). AJ acknowledges the Welsh Government for a Ser

Cymru II Award (80762-CU-063).

References

1. C. E. Badr, Ed., *Bioluminescent Imaging*, Humana Press, Totowa, NJ (2014).
2. A. Rehemtulla et al., “Rapid and quantitative assessment of cancer treatment response using in vivo bioluminescence imaging,” Neoplasia **2**(6), 491–495 (2000).
3. D.-E. Kim et al., “Imaging of stem cell recruitment to ischemic infarcts in a murine model,” Stroke **35**(4), 952–957 (2004).
4. F. Sher et al., “Bioluminescence imaging of Olig2-neural stem cells reveals improved engraftment in a demyelination mouse model,” Stem Cells **27**(7), 1582–1591 (2009).
5. A. Tennstaedt et al., “Noninvasive Multimodal Imaging of Stem Cell Transplants in the Brain Using Bioluminescence Imaging and Magnetic Resonance Imaging,” in Methods in Molecular Biology, pp. 153–166 (2013).
6. C. Vandeputte et al., “Bioluminescence imaging of stroke-induced endogenous neural stem cell response,” Neurobiol. Dis. **69**, 144–155 (2014).
7. J. Adamczak et al., “Neurogenesis upregulation on the healthy hemisphere after stroke enhances compensation for age-dependent decrease of basal neurogenesis,” Neurobiol. Dis. **99**, 47–57 (2017).
8. S. Iwano et al., “Single-cell bioluminescence imaging of deep tissue in freely moving animals,” Science **359**(6378), 935–939 (2018).
9. M. Aswendt et al., “Boosting bioluminescence neuroimaging: an optimized protocol for brain studies,” PLoS One **8**(2), e55662 (2013).
10. S. Vogel et al., “Initial graft size and not the innate immune response limit survival of engrafted neural stem cells,” J. Tissue Eng. Regen. Med. **12**(3), 784–793 (2018).
11. J. R. de Wet et al., “Firefly luciferase gene: structure and expression in mammalian cells,” Mol. Cell. Biol. **7**(2), 725–737 (1987).
12. A. Tennstaedt et al., “Human neural stem cell intracerebral grafts show spontaneous early neuronal differentiation after several weeks,” Biomaterials **44**, 143–154 (2015).
13. C. Daniel et al., “Dual-Color Bioluminescence Imaging for Simultaneous Monitoring of the Intestinal Persistence of Lactobacillus plantarum and Lactococcus lactis in Living Mice,” Appl. Environ. Microbiol. **81**(16), 5344–5349 (2015).
14. C. A. Maguire et al., “Triple bioluminescence imaging for in vivo monitoring of cellular processes,” Mol. Ther. Nucleic Acids **2**, e99 (2013).
15. L. Mezzanotte et al., “A new multicolor bioluminescence imaging platform to investigate NF-κB activity and apoptosis in human breast cancer cells,” PLoS One **9**(1), e85550 (2014).
16. S. T. Gammon et al., “Spectral unmixing of multicolored bioluminescence emitted from heterogeneous biological sources,” Anal. Chem. **78**(5), 1520–1527 (2006).
17. S. K. Cool et al., “Comparison of in vivo optical systems for bioluminescence and fluorescence imaging,” J. Fluoresc. **23**(5), 909–920 (2013).
18. B. R. Branchini et al., “Red- and green-emitting firefly luciferase mutants for bioluminescent reporter applications,” Anal. Biochem. **345**(1), 140–148 (2005).
19. B. R. Branchini et al., “Thermostable red and green light-producing firefly luciferase mutants for bioluminescent reporter applications,” Anal. Biochem. **361**(2), 253–262 (2007).
20. G. H. E. Law et al., “Mutagenesis of solvent-exposed amino acids inPhotinus pyralisluciferase improves thermostability and pH-tolerance,” Biochem. J **397**(2), 305–312 (2006).
21. A. Jathoul et al., “Development of a pH-Tolerant Thermostable Photinus pyralis Luciferase for Brighter In Vivo Imaging,” in Bioluminescence - Recent Advances in Oceanic Measurements and Laboratory Applications, D. Lapota, Ed., InTech (2012).
22. G. H. E. Law et al., “Mutagenesis of solvent-exposed amino acids in Photinus pyralis

luciferase improves thermostability and pH-tolerance," Biochem. J **397**(2), 305–312 (2006).
23. B. R. Branchini et al., "Red-emitting luciferases for bioluminescence reporter and imaging applications," Anal. Biochem. **396**(2), 290–297 (2010).
24. H. Zhao et al., "Emission spectra of bioluminescent reporters and interaction with mammalian tissue determine the sensitivity of detection in vivo," J. Biomed. Opt. **10**(4), 41210 (2005).
25. S. Bhaumik and S. S. Gambhir, "Optical imaging of Renilla luciferase reporter gene expression in living mice," Proceedings of the National Academy of Sciences **99**(1), 377–382 (2001).
26. L. Mezzanotte et al., "Evaluating reporter genes of different luciferases for optimized in vivo bioluminescence imaging of transplanted neural stem cells in the brain," Contrast Media Mol. Imaging **8**(6), 505–513 (2013).
27. M. Hampf and M. Gossen, "A protocol for combined Photinus and Renilla luciferase quantification compatible with protein assays," Anal. Biochem. **356**(1), 94–99 (2006).
28. C. Ran and A. Moore, "Spectral unmixing imaging of wavelength-responsive fluorescent probes: an application for the real-time report of amyloid Beta species in Alzheimer's disease," Mol. Imaging Biol. **14**(3), 293–300 (2012).
29. T. Zimmermann, "Spectral imaging and linear unmixing in light microscopy," Adv. Biochem. Eng. Biotechnol. **95**, 245–265 (2005).
30. L. Mezzanotte et al., "Evaluating reporter genes of different luciferases for optimized in vivo bioluminescence imaging of transplanted neural stem cells in the brain," Contrast Media Mol. Imaging **8**(6), 505–513 (2013).
31. A. P. Jathoul et al., "A dual-color far-red to near-infrared firefly luciferin analogue designed for multiparametric bioluminescence imaging," Angew. Chem. Int. Ed Engl. **53**(48), 13059–13063 (2014).
32. Y. Liang, P. Walczak, and J. W. M. Bulte, "Comparison of red-shifted firefly luciferase Ppy RE9 and conventional Luc2 as bioluminescence imaging reporter genes for in vivo imaging of stem cells," J. Biomed. Opt. **17**(1), 016004 (2012).
33. L. Mezzanotte et al., "Sensitive dual color in vivo bioluminescence imaging using a new red codon optimized firefly luciferase and a green click beetle luciferase," PLoS One **6**(4), e19277 (2011).
34. E. Michelini et al., "Spectral-Resolved Gene Technology for Multiplexed Bioluminescence and High-Content Screening," Anal. Chem. **80**(1), 260–267 (2008).
35. S. Pesnel et al., "Quantitation in bioluminescence imaging by correction of tissue absorption for experimental oncology," Mol. Imaging Biol. **13**(4), 646–652 (2011).
36. K. A. Feeney et al., "In-depth Characterization of Firefly Luciferase as a Reporter of Circadian Gene Expression in Mammalian Cells," J. Biol. Rhythms **31**(6), 540–550 (2016).
37. B. Philip et al., "A highly compact epitope-based marker/suicide gene for easier and safer T-cell therapy," Blood **124**(8), 1277–1287 (2014).
38. S. K. Dhara and S. L. Stice, "Neural differentiation of human embryonic stem cells," J. Cell. Biochem. **105**(3), 633–640 (2008).

Figure legends

Fig. 1: Comparison of Luc2, CBG99, PpyRE9, x5g, x5r, and hRluc emission specra in vitro. Plotted is the photon emission from EF1α-luciferase-T2A-copGFP transfected HEK 293T cells recorded with the IVIS Spectrum CT system (mean of n=4-6). Photon emission was normalized to the individual copGFP expression. Graph with grey background is a zoom-in for 580-700 nm to highlight differences in the red part of the spectra.

Fig. 2. Unmixing of x5g and x5r luciferases expressed by HEK 293T cells. (a) Fluorescence microscopy overlay with phase contrast image of cells at 2 days post transfection, used for the unmixing experiment (scale bar 25 µm). (b) Unmixed spectra of x5r and x5g calculated by the unmixing algorithm. (c) Plating scheme for x5g and x5r cells in different numbers (n=3) and the corresponding false-colored unmixed result displayed as green/red composite as well as the open filter, x5g, and x5 red unmixed images. (d) Plot of measured unmixed x5g and x5r photon flux plotted vs. the plated ratio of x5g cells in the mix (n=3). Linear fitting for both luciferases underlines high accuracy of unmixed values with plated cells.

Fig. 3: In vitro modeling of superficial vs. deep x5g and x5r Fluc sources with tissue-like agarose. (a) Different volumes of tissue-like agarose were placed above the HEK 293T cell layer to mimic overlaying tissue in different thickness. Micrographs represent selected bioluminescence/photo overlays from the x5g and x5r unmixing, respectively. (b) Quantitative analysis and polynomial fit for the decreasing photon emission, detected when more blood agar volume was added.

Fig. 4: In vivo emission spectra of x5g and x5r in comparison to Luc2, CBG99, PpyRE9, and hRluc expressed in mammalian cells implanted in the mouse brain (data in part adapted from our previous publication comparing different luciferases [26]).

Fig. 5. Spectral unmixing efficiently determines x5g/r cell ratios in vivo. Transiently transfected HEK 293T cells expressing x5g or x5r luciferases were transplanted into the cortex **(a)** or striatum **(d)** and bioluminescence imaging was applied 1 day later. Non-normalized spectra from the x5g and x5r cells differ, dependent on transplantation depth: cortex **(b)**, striatum **(e)**. Spectral unmixing of x5g ratio is in good agreement with expected (dotted line) x5g ratio for the cortical **(c)** as well as striatal **(f)** grafts. Significant differences are highlighted by asterisks.

Fig. 6. Spectral unmixing of two neural stem cell (NSC) populations. (a) NSC lines expressing x5g or Luc2 were implanted in different ratios into the cortex of nude mice. **(b)** Quantitative analysis of spectral unmixing from imaging data acquired 1 day and 2 days post implantation (dpi). **(c)** Representative immunohistochemical staining of an NSC graft (EF1α-Luc2-T2A-copGFP). Human nuclei (HuNu) to discriminate the human cell graft in the mouse brain. Enhanced copGFP with anti-copGFP antibody to visualize transplanted cells expressing the transgene. Hoechst to visualize cell nuclei. Scale bar

752 50 um.
753

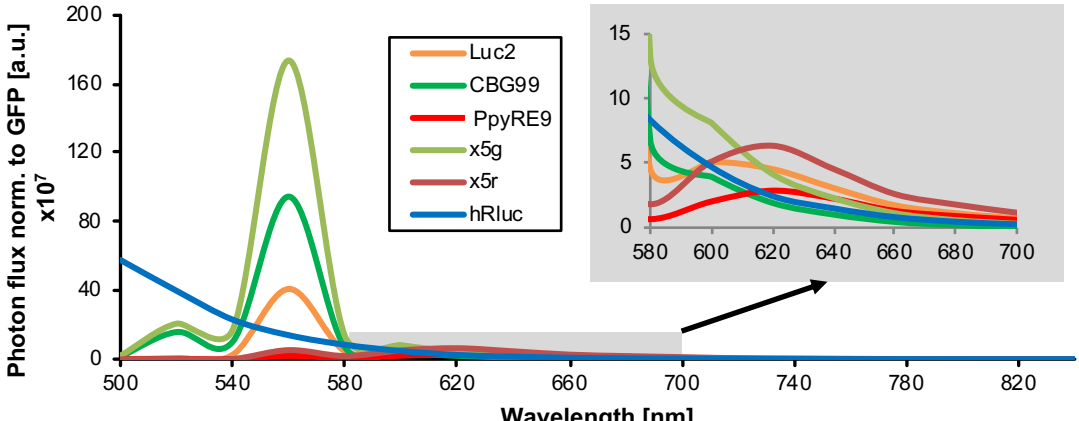
Photon flux norm. to GFP [a.u.]
x10^7
200
160
120
80
40
0
500
540
580
620
660
700
740
780
820
Wavelength [nm]
Luc2
CBG99
PpyRE9
x5g
x5r
hRluc
15
10
5
0
580
600
620
640
660
680
700

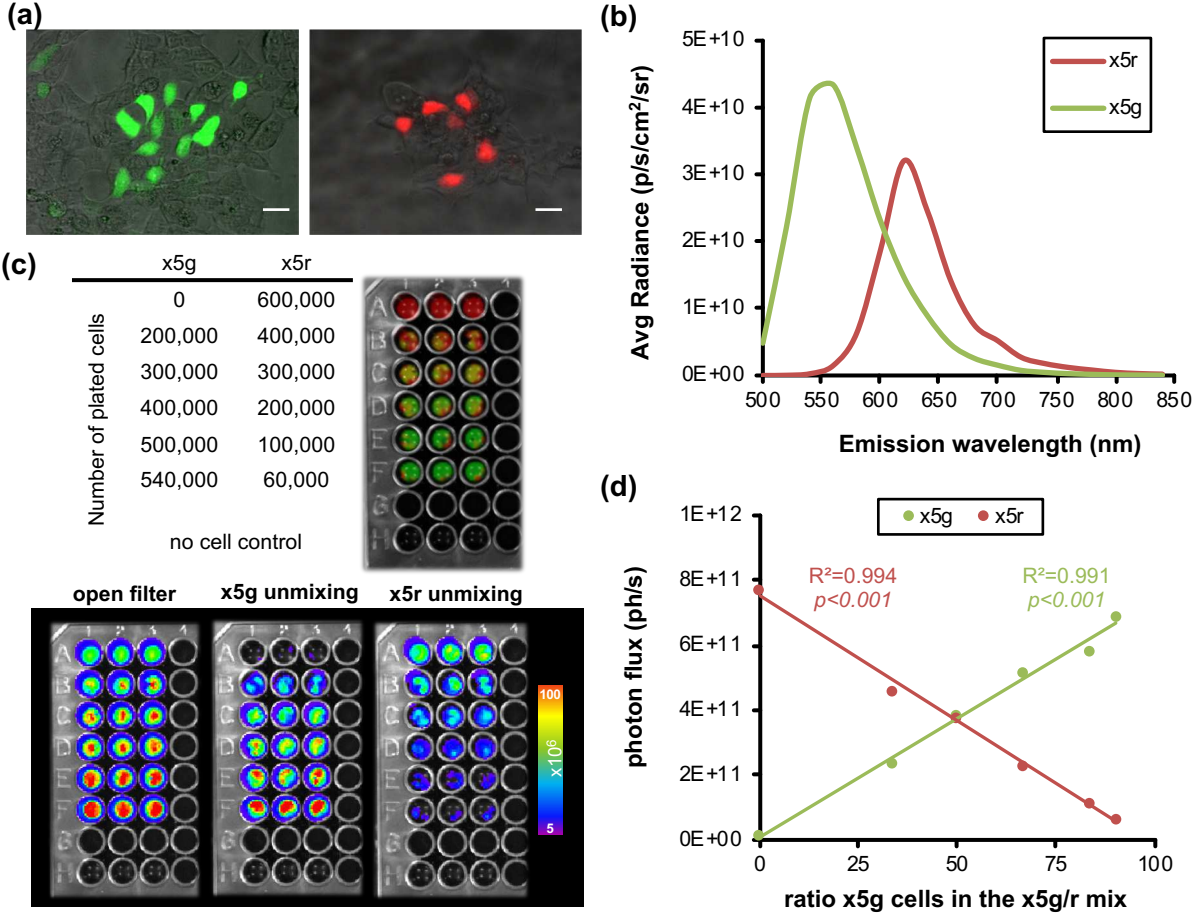
(a)
(b)
5E+10
4E+10
3E+10
2E+10
1E+10
0E+00
Avg Radiance (p/s/cm²/sr)
x5r
x5g
500
550
600
650
700
750
800
850
Emission wavelength (nm)
(c)
x5g
x5r
Number of plated cells
0
600,000
200,000
400,000
300,000
300,000
400,000
200,000
500,000
100,000
540,000
60,000
no cell control
open filter
x5g unmixing
x5r unmixing
100
x10⁶
5
(d)
1E+12
8E+11
6E+11
4E+11
2E+11
0E+00
photon flux (ph/s)
x5g
x5r
R²=0.994
p<0.001
R²=0.991
p<0.001
0
25
50
75
100
ratio x5g cells in the x5g/r mix

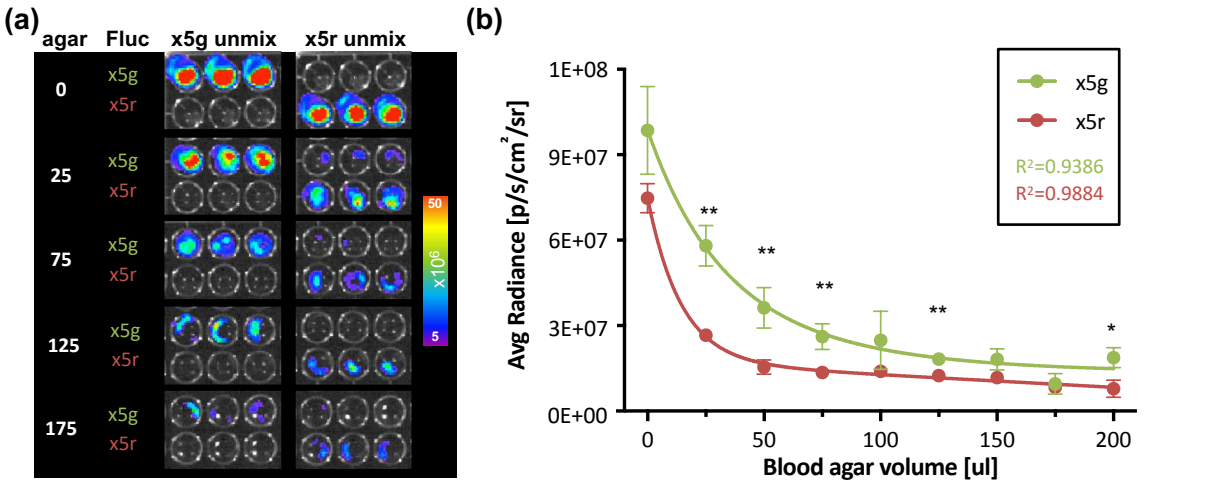
(a)
agar
Fluc
x5g unmix
x5r unmix
0
25
75
125
175
x5g
x5r
50
x10^6
5
(b)
1E+08
9E+07
6E+07
3E+07
0E+00
Avg Radiance [p/s/cm²/sr]
0
50
100
150
200
Blood agar volume [ul]
x5g
x5r
R²=0.9386
R²=0.9884
**
**
**
**
*

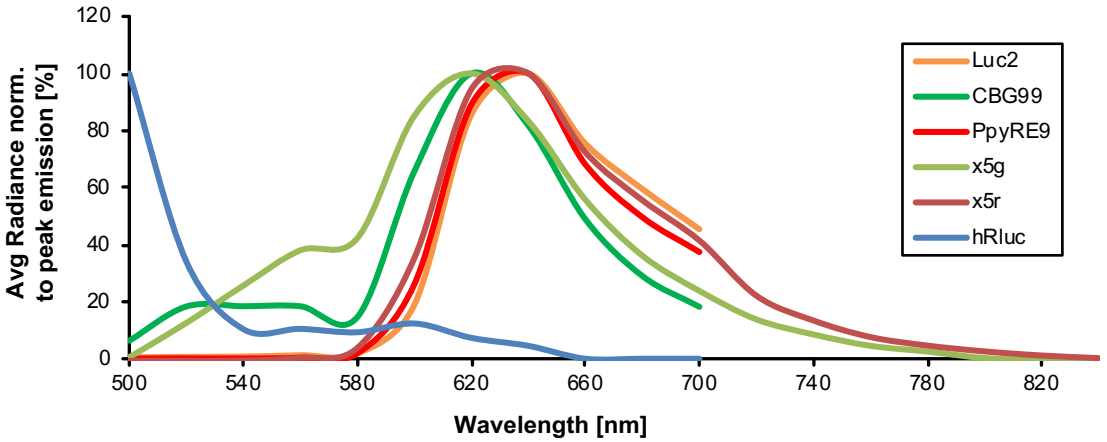
Avg Radiance norm. to peak emission [%]
120
100
80
60
40
20
0
500
540
580
620
660
700
740
780
820
Wavelength [nm]
Luc2
CBG99
PpyRE9
x5g
x5r
hRluc

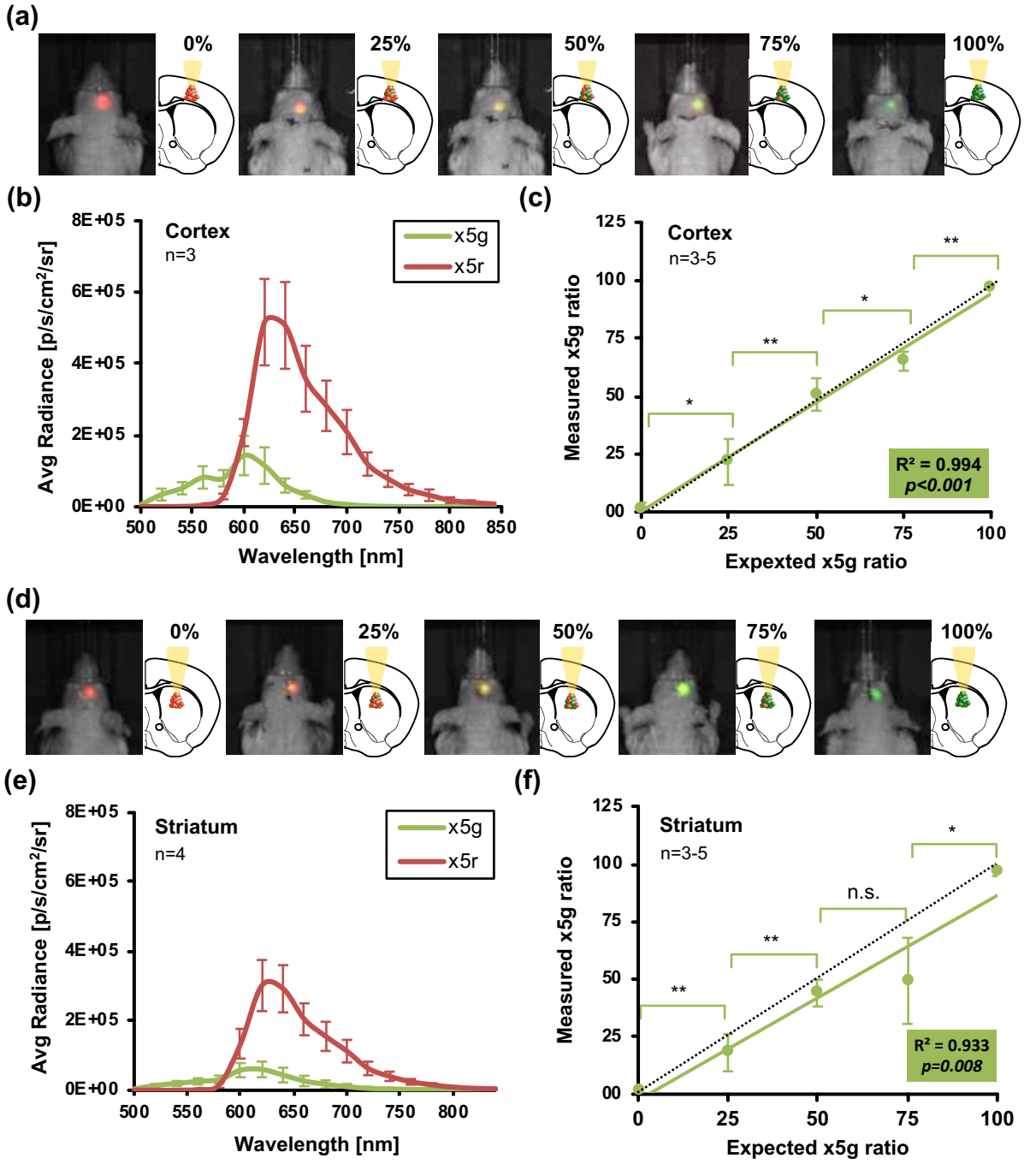
(a)
0%
25%
50%
75%
100%
(b)
Cortex
n=3
x5g
x5r
Avg Radiance [p/s/cm²/sr]
8E+05
6E+05
4E+05
2E+05
0E+00
500
550
600
650
700
750
800
850
Wavelength [nm]
(c)
Cortex
n=3-5
Measured x5g ratio
125
100
75
50
25
00
0
25
50
75
100
Expexted x5g ratio
*
**
*
**
R² = 0.994
p<0.001
(d)
0%
25%
50%
75%
100%
(e)
Striatum
n=4
x5g
x5r
Avg Radiance [p/s/cm²/sr]
8E+05
6E+05
4E+05
2E+05
0E+00
500
550
600
650
700
750
800
Wavelength [nm]
(f)
Striatum
n=3-5
Measured x5g ratio
125
100
75
50
25
00
0
25
50
75
100
Expected x5g ratio
**
**
n.s.
*
R² = 0.933
p=0.008

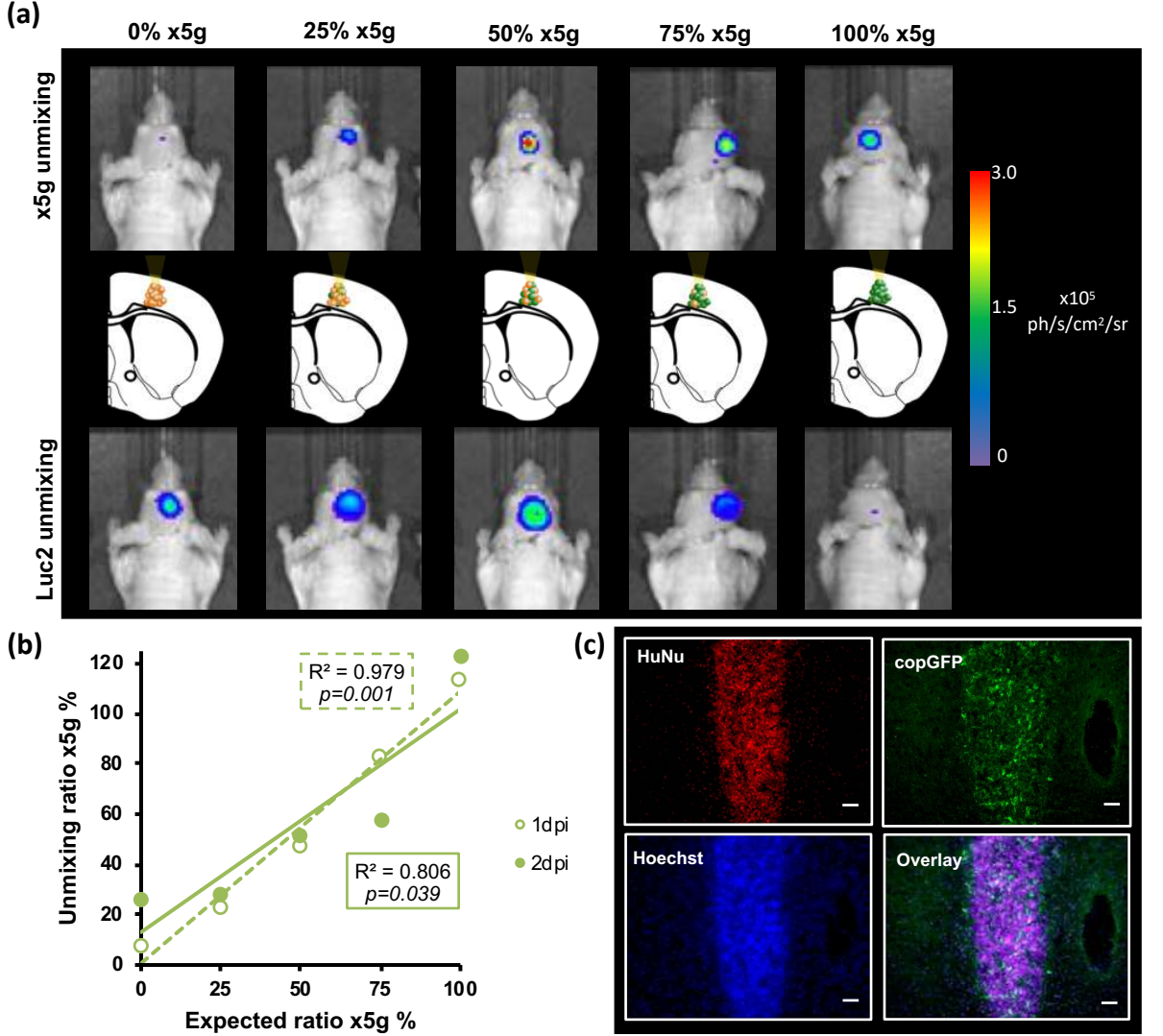
(a)
0% x5g
25% x5g
50% x5g
75% x5g
100% x5g
x5g unmixing
Luc2 unmixing
3.0
1.5
0
x10⁵
ph/s/cm²/sr
(b)
Unmixing ratio x5g %
Expected ratio x5g %
R² = 0.979
p=0.001
R² = 0.806
p=0.039
1dpi
2dpi
(c)
HuNu
copGFP
Hoechst
Overlay